Journal of Materials Chemistry B

PAPER

View Article Online
View Journal | View Issue

Cite this: J. Mater. Chem. B, 2023, 11, 6896

Agar/gelatin hydro-film containing EGF and Aloe vera for effective wound healing†

Itxaso Garcia-Orue,‡[abc] Edorta Santos-Vizcaino, ‡[abc] Jone Uranga,[d] Koro de la Caba,[de] Pedro Guerrero, *[def] Manoli Igartua[abc] and Rosa Maria Hernandez *[abc]

In the current study, we produced a hydro-film dressing for the treatment of chronic wounds. The hydro-film structure was composed of gelatin cross-linked with citric acid, agar and Aloe vera extract (AV); additionally epidermal growth factor (EGF) was loaded to promote wound healing. Due to the excellent hydrogel-forming ability of gelatin, the obtained hydro-film was able to swell 884 ± 36% of its dry weight, which could help controlling wound moisture. To improve gelatin mechanical properties, polymer chains were cross-linked with citric acid and agar, reaching an ultimate tensile strength that was in the highest range of human skin. In addition, it showed a slow degradation profile that resulted in a remaining weight of 28 ± 8% at day 28. Regarding, biological activity, the addition of AV and citric acid provided the ability to reduce human macrophage activation, which could help reverse the permanent inflammatory state of chronic wounds. Moreover, loaded EGF, together with the structural AV of the hydro-film, promoted human keratinocyte and fibroblast migration, respectively. Furthermore, the hydro-films presented excellent fibroblast adhesiveness, so they could be useful as provisional matrices for cell migration. Accordingly, these hydro-films showed suitable physicochemical characteristics and biological activity for chronic wound healing applications.

Received 25th December 2022,
Accepted 21st June 2023

DOI: 10.1039/d2tb02796h

rsc.li/materials-b

Introduction

In recent years, chronic wounds have become a challenging clinical problem, since their prevalence is growing exponentially along with the increase of their predisposing factors such as, ageing, diabetes and obesity. In fact, non-healing chronic wounds have a prevalence rate of 2% in the USA,[1,2] and they impact greatly in patients life quality, due to frequent hospitalizations, infections and even mortality.[3] In a study conducted in 2018, it was stated that wounds affect about 15% of the beneficiaries of the USA Medicare service (8.2 million patients), causing an estimate annual cost of $28 billion.[1] However, current treatments cannot guarantee an effective healing and, thus, multiple researches are focused on the search for new wound dressings. The challenges that these researches face are not only related to the development of an effective dressing; an ideal dressing also needs to be cost-effective, completely characterized to ensure its safety, well tolerated and comfortable for the patients.

Among the wide variety of proteins used for wound healing, gelatin needs to be highlighted. It is a protein extracted from collagen, the main component of the extracellular matrix (ECM) of the dermis,[4] and both collagen and gelatin have been extensively used in wound healing, due to their biocompatibility and biodegradability. In addition, they mimic the structure of the ECM and their chains contain arginine–glycine–aspartic (RGD) motifs, an amino acid sequence involved in cell adhesion. Those properties give collagen and gelatin an improved behavior for wound healing, since they can act as a provisional matrix for cell migration.[5,6] Moreover, gelatin presents some advantages in comparison to collagen, such as a less expensive and less antigenic nature, since it is partially denatured.[7,8]

Gelatin is able to form hydrogels and hydro-films due to its capacity to absorb large volumes of water. The use of those hydro-films as wound dressings presents several advantages,

[a] NanoBioCel Research Group, Laboratory of Pharmaceutics, School of Pharmacy, University of the Basque Country (UPV-EHU), Vitoria-Gasteiz, Spain. E-mail: rosa.hernandez@ehu.eus
[b] Biomedical Research Networking Centre in Bioengineering, Biomaterials and Nanomedicine (CIBER-BBN). Institute of Health Carlos III, Madrid, Spain
[c] Bioaraba, NanoBioCel Research Group, Vitoria-Gasteiz, Spain
[d] BIOMAT Research Group, University of the Basque Country (UPV/EHU), Escuela de Ingeniería de Gipuzkoa, Plaza de Europa 1, 20018 Donostia-San Sebastián, Spain. E-mail: pedromanuel.guerrero@ehu.eus
[e] BCMaterials, Basque Center for Materials, Applications and Nanostructures, UPV/EHU Science Park, 48940, Leioa, Spain
[f] Proteinmat materials SL, Avenida de Tolosa 72, 20018 Donostia-San Sebastian, Spain

† Electronic supplementary information (ESI) available. See DOI: https://doi.org/10.1039/d2tb02796h

‡ These authors contributed equally to this work.

among which their ability to control wound moisture can be highlighted. In this regard, in exudative wounds hydro-films are able to absorb excess fluid from wound, preventing the wounds from macerating. On the other hand, hydro-films are able to release water to prevent non-exudative wounds from drying out.[6] Furthermore, hydro-films have a certain similarity to an artificial skin, due to their elastic and resistant nature, that create a barrier permeable for gas exchange, while impermeable for microorganisms. In addition, transparent hydro-films allow wound monitoring without the removal of the dressing, which make them comfortable for the patient.[9]

However, the hydrophilicity of gelatin is also its main weakness, since it dissolves in water at temperatures above 35 °C.[10] Therefore, cross-linking of its protein chains is necessary to maintain the mechanical properties *in vivo*. The cross-linking method and degree determines the form that gelatin adopts, which ranges from amorphous gels to semi-stiff sheets, such as the hydro-films developed in the current study.[11] Another strategy to improve gelatin's mechanical properties is to combine it with a polymer with a stiffer nature, such as agar, a phycocolloid extracted from red algae that has excellent gel-forming abilities, and is characterized by high-temperature resistance and high mechanical strength.[12]

In addition, gelatin dressings allow the encapsulation of bioactive compounds that can accelerate the healing process, including compounds able to reduce the perpetual inflammatory state of chronic wounds. In that regard, the inclusion of Aloe vera plant extract in the structure of the hydro-film (AV) can be a suitable strategy, since it presents anti-inflammatory activity related to the inhibition of pro-inflammatory cytokines, reactive oxygen species (ROS) and the JAK1-STAT1/3 pathway. Moreover, AV has proliferative properties, through the up-regulation of the vascular endothelial growth factor (VEGF-A), the transforming growth factor-β1 (TGF-β1) and the basic fibroblast growth factor (bFGF) expression in fibroblasts, overall promoting tissue regeneration.[13,14] Therefore, AV has been used to treat skin wounds since ancient times, and recent researches have confirm its effectiveness. In that regard, AV has been included in electrospun nanofibers,[15,16] hydrogels,[17,18] membranes,[19,20] sponges[21,22] and fabrics[23] with proven efficacy in wound healing.

Moreover, the dressings can protect bioactive compounds from external harm and achieve a sustained release. This is interesting for compounds with short stability *in vivo*, as the epidermal growth factor (EGF), a growth factor involved in the healing process that is downregulated in chronic wounds.[24] Concretely, EGF plays a key role promoting dermal regeneration by stimulating the migration and proliferation of keratinocytes, endothelial cells and fibroblasts, and thus enhancing epidermal regeneration, granulation tissue formation and angiogenesis, and overall promoting wound closure.[25,26] In fact, its exogenous administration has reported to be effective in chronic and burn wounds.[27–29]

Taking all that into account, the aim of the current study was to develop a gelatin hydro-film with improved mechanical properties and efficacy for the treatment of chronic wounds. To accomplish the first goal, agar was included in the formulation and gelatin was cross-linked with citric acid. On the other hand, to enhance the wound healing effect, AV and EGF were added to the formulation. After developing the hydro-films, we performed a physicochemical characterization to test their suitability as wound dressings and their ability to release EGF in a sustained way. Then, we assessed their bioactivity through anti-inflammatory and wound closure studies. The obtained results showed that the developed dressing had suitable mechanical and swelling properties for wound healing that allowed easy handling and adequate moisture control. In addition, due to the inclusion of AV and citric acid, hydro-films were able to inhibit the inflammatory response, which is persistent in chronic wounds. Moreover, the hydro-films promoted the migration of both fibroblasts and keratinocytes, which is necessary for wound closure and reepithelization, thanks to the addition of AV and EGF.

Results and discussion

The aim of the current study was to develop an agar/gelatin hydro-film cross-linked with citric acid containing loaded EGF and structural AV as bioactive ingredients. In a first step to achieve this goal, we developed hydro-films without both active compounds (G hydro-films), or without EGF (GA hydro-films), to characterize their suitability for wound healing prior to EGF addition. GAE hydro-films physicochemical properties were not characterized, since the addition of EGF dropwise onto GA hydro-films does not alter the chemical structure of the hydro-film, as they interact solely through polyion complexes.

The hydro-films were easily manageable, as they could be held with tweezers (as observed in Fig. 1A), which eases their application and removal. In addition, they were thin and transparent, which could be useful in wound healing to monitor underneath tissue with no need to remove the dressing, and thus avoiding the damage and pain that dressing removal inflicts.[30]

Fourier transform infrared (FTIR) spectroscopy

FTIR spectra of G and GA hydro-films were analyzed in comparison to that of pure gelatin to evaluate the interactions between the components of the hydro-film. Hydro-films presented a characteristic broad absorption band around 3500–3000 cm^{-1} (data not shown), attributed to the free and bounded –NH and –OH. As shown in Fig. 1B, with the addition of citric acid and agar, the characteristic absorption bands of gelatin, associated with the amide I band (C═O stretching) at 1627 cm^{-1} and with the amide II band (N–H bending) at 1529 cm^{-1}, shifted to 1637 cm^{-1} and 1549 cm^{-1}, respectively. Additionally, the characteristic band of citric acid at 1743 cm^{-1}, assigned to the C═O stretching of citric acid, was not present in the spectra of the hydro-films, which was an indicative of the cross-linking reaction of citric acid with the amino groups of gelatin.[31] Moreover, the absorption band at 1081 cm^{-1} (C–O stretching), attributed to glycerol, shifted to 1041 cm^{-1} with the addition of agar.

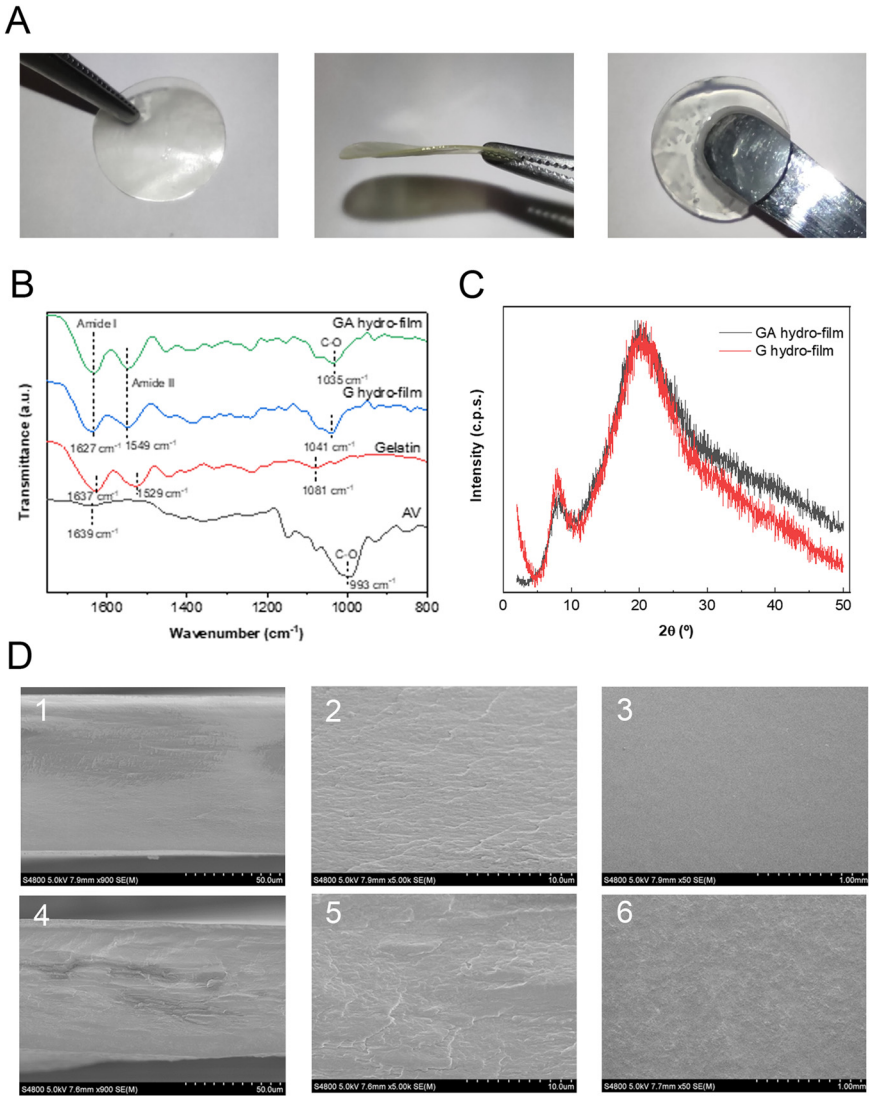

Fig. 1 Structure of G and GA hydro-films. (A) Macroscopic photographs of GA hydro-films. (B) FTIR spectra. (C) XRD patterns. (D) SEM images (1, 2 and 3 correspond to G hydro-films; 4, 5 and 6 correspond to GA hydro-films; 1, 2, 4 and 5 correspond to the hydro-film cross-section; 3 and 6 correspond to the hydro-film surface).

The shift of the bands indicated physical interactions among the components of the hydro-films, which were favored by the temperature used during the film preparation and led to easy to handle hydro-films and to an improvement of the hydro-film behavior in PBS at 37 °C.

The spectrum of AV showed some characteristic bands: the band at 1639 cm^{-1}, attributed to C=O stretching, and the bands in the region between 1200 and 850 cm^{-1}, assigned to C–O stretching.

X-Ray diffraction (XRD)

The crystalline/amorphous nature of hydro-films was assessed by XRD and hydro-film patterns are shown in Fig. 1C. All hydro-films exhibited a diffraction peak around 8°, related to the remaining triple-helix structure of collagen.[32] The addition of AV caused a slight decrease in the intensity of this peak, since new hydrogen bonds were formed between the hydroxyl groups of AV and the polar groups of gelatin. Additionally, all hydro-films showed a second wide peak located around 21°, related to the single left-handed helix chain of gelatin. It is worth highlighting that the characteristic peak of agar around 13.9° was not observed, due to changes in the crystalline structure of the polymeric chains caused by the interactions among the components of the hydro-film.[33]

Scanning electron microscopy (SEM)

The hydro-films cross-sections (Fig. 1D 1 and 2 and 4 and 5) and surface (Fig. 1D 3 and 6) were analyzed by SEM. In general, hydro-films were compact and homogeneous, without pores or aggregations, as shown in Fig. 1D for G hydro-films (images 1 and 2) and for GA hydro-films (images 4 and 5). This homogeneous structure indicated a good distribution of AV into the hydro-films and a good compatibility between all the components. Moreover, the addition of AV increased the hydro-films

surface roughness (image 6), which could play a positive role in wound healing, since rougher morphologies increase the specific surface area and enhance the adhesion of erythrocytes and platelets, which lead to a more effective aggregation of red blood cells and thus achieving a hemostatic effect.[34]

Water uptake

Continuing the characterization, we analyzed the swelling ability of the hydro-films, which determines their capacity to absorb water and, thus, to control the moisture content of the wound bed. Dry wounds need external hydration, so wet hydro-films could be useful since they are able to release water. On the contrary, in exudative wounds the excessive exudate needs to be removed to avoid wound maceration, which could be achieved applying dry hydro-films that can absorb large volumes of water.[35]

Regarding water uptake, Fig. 2A shows that both hydro-films reached a similar water uptake at 24 h, 930.7 ± 66.8% and 884 ± 36.4% for G and GA hydro-films, respectively. However, GA hydro-films presented a quicker water uptake, since their

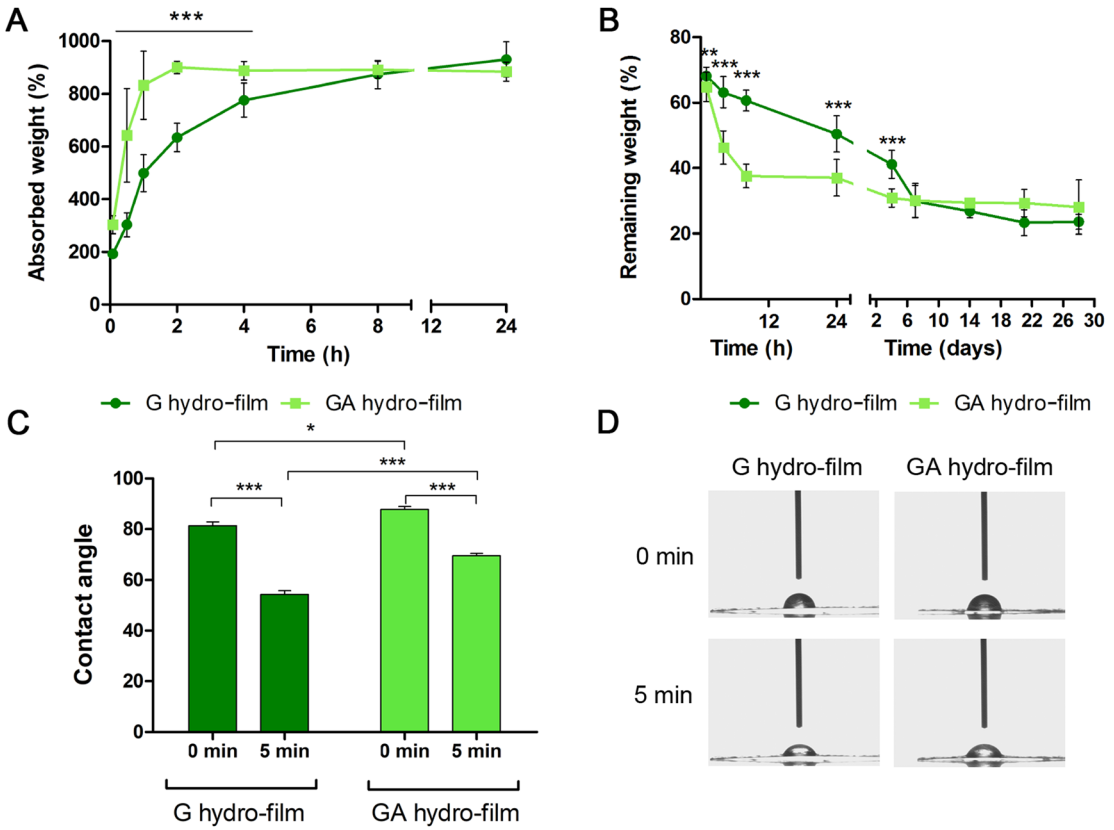

E

Hydro-film	WVTR (g/m²day)	EM (MPa)	TS (MPa)	EAB (%)
G	1522 ± 55[a]	198 ± 24[a]	27 ± 2[c]	45 ± 4[c]
GA	1479 ± 38[a]	361 ± 8[b]	31 ± 2[d]	36 ± 4[d]

Different superscripts within a column indicate statistically significant different values ([a-b] ***p<0.001 and [c-d] **p<0.01).

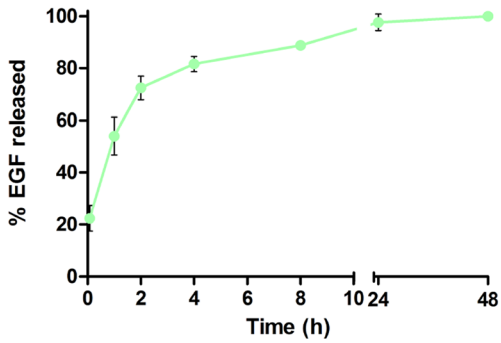

Fig. 2 Characterization of G and GA hydro-films. (A) Water uptake of G and GA hydro-films. We gave the results as mean ± SD of the percentage of water absorbed in comparison to the dry hydro-films. ***$p < 0.001$ among groups. (B) Hydro-films degradation in an aqueous medium. Results are displayed as mean ± SD of the remaining weight (%). ** $p < 0.01$ and ***$p < 0.001$ among groups. (C) Hydro-films contact angle at time 0 and time 5 min. Results are expressed as mean ± SD. * $p < 0,05$,. ** $p < 0.01$ and ***$p < 0.001$ among groups. (D) Contact angle images of the hydro-films at time 0 ant time 5 min. (E) Water vapor transmission rate (WVTR), elastic modulus (EM), tensile strength (TS), and elongation at break (EAB) values. We expressed all the results as mean ± SD. (F) EGF release from GAE hydro-films. Results are displayed as mean ± SD of the percentage of EGF released from the hydro-film.

percentage of swelling was significantly higher than that of G hydro-films from the beginning of the study until 4 h. That difference was likely attributed to the interference of Aloe vera in the gelatin crosslinking process, creating steric hindrance and thereby leaving more spaces for water penetration. The faster water uptake of GA hydro-films could lead to a faster absorption of wound exudate and, thus, to a faster control of wound moisture.

In addition, the effect of pH on the swelling of the hydro-films was analyzed (Fig. 1A and B). The results showed that there were no differences in the water uptake of G and GA hydro-films immersed in buffers with pH 5 and pH 8 at any time point. Water uptake at 72 h was 1044 ± 156, 1022 ± 55%, 1097 ± 81% and 1132 ± 50%, for G hydro-films at pH 5 and 8 and GA hydro-films at pH 5 and 8, respectively.

Aqueous degradation

Hydro-films degradation in an aqueous medium (Fig. 2B) followed a similar pattern to water uptake, since both hydro-films presented a similar degradation value at the end of the study, although the degradation occurred faster for GA hydro-film. Since the beginning of the study until day 1, GA hydro-films showed a significantly lower weight, and from day 4 onwards, the remaining weight did not show statistic differences between both hydro-films. In fact, at day 28, the remaining weight of G hydro-films was 23.5 ± 2.3% and that of GA hydro-films was 28.1 ± 8.3%. The faster weight loss occurred in GA hydro-films could be due to decreased crosslinking caused by the steric impediment that AV presented in the preparation process. Moreover, it could be an indicator of AV release, a step needed for AV to exert its bioactivity. Noteworthy, Baghersad *et al.* observed an increased rate of hydrolytic degradation in gelatin-polycaprolactone electrospun scaffolds upon AV addition.[16]

As can be seen in Fig. 1C, the solubility of G hydro-films is affected by pH, and G hydro-films at pH 8 showed a lower remaining weight than at pH 5. This occurred since the closer the pH is to the isoelectric point of gelatin (pH 9), the ionization grade of gelatin is lower and thus the physical electrostatic interaction between the gelatin and agar decreased. This leads to a weaker net of polymer that allows the entry of water, favoring the hydrolytic degradation.

Contact angle

The surface wettability of the films was determined by analyzing the behavior of the water droplet on the film surface at different times. The wettability of G and GA films (Fig. 2C and D) followed a similar pattern with time, as both films showed a decrease in contact angle with time. G films had a contact angle of 81.4 ± 3.5, which decreased to 54.3 ± 3.7 after 5 min; GA films had slightly higher contact angle values, 87.8 ± 2.9 (t = 0) and 69.6 ± 2.3 (t = 5 min).

Water vapor transmission rate (WVTR)

The WVTR of a dressing also conditions the moisture content of the wound, since a low WVTR can cause accumulation of exudate and a high WVTR an overly fast drying.[36] Therefore, commercial dressings have a wide variety of WVTR values, depending on the type of wound that are aimed to, ranging from 90 to 3350 g m^{-2} day^{-1}.[37] The results obtained with G and GA hydro-films, 1522 ± 55 and 1479 ± 38 g m^{-2} day^{-1}, respectively (Fig. 2E), were in the middle of those values, suggesting that these hydro-films could be useful for wounds with a moderate exudative nature.

Mechanical properties

As wound dressings, the hydro-films will be in close contact with the skin, and must be able to stretch with it without tearing apart.[38] Thereby, we determined their mechanical properties (Fig. 2E), and we observed that the ultimate tensile strength (27.66 ± 2.01 MPa and 31 ± 2 MPa for G and GA hydro-films, respectively) was in the highest range of human skin tensile strength (1 to 32 MPa), highlighting the optimal mechanical properties of the hydro-films.[39]

Regarding the elastic modulus, the values were 198.12 ± 16.16 MPa and 360.66 ± 7.82 MPa for G and GA hydro-films, respectively. In addition, the incorporation of AV affected the deformation of the hydro-films. G hydro-films showed an elongation at breakage of 45.26 ± 4.38%, while GA hydro-filmspresented a lower value of 35.97 ± 4.16%, in accordance with the increase in the tensile strength observed.

Therefore, the addition of AV increased the elastic moduli and the tensile strength, while decreasing the flexibility by reducing the elongation at break. This effect may be related to complexation or cross-linking, as suggested by a couple of studies where a slight increase of the tensile strength was observed upon AV addition to fish gelatin based films[40] and to PLGA electrospun membranes.[41]

EGF release

Once we characterized the physical and chemical properties of the hydro-films and determined their suitability for wound healing, we poured EGF dropwise onto GA dry hydro-films to prepare GAE hydro-films. We chose this inclusion method to protect EGF, because the temperatures used during the hydro-film preparation could lead to EGF denaturalization due to its protein nature. Even so, we expected a sustained release driven by the formation of polyion complexes between the positively charged hydro-film and the negatively charged EGF. It is important to remark that the polyion complexion could be able to protect EGF from denaturation and enzymatic degradation *in vivo*, until its release from the hydro-film.[42]

In this case, the sustained release presented a biphasic profile (Fig. 2F) that had an initial burst in the first 2 h where 72.4 ± 4.5% of the total EGF content was released; and a posterior slower release phase that achieved a complete EGF release in 48 h. A method to decrease the burst release could be the conjugation of the amino groups of basic residues in gelatin with ethylenediamine as described by Hori *et al.* This way cationized gelatin was obtained, which presented a smaller burst release but also an inferior total cumulative release of EGF.[27]

Hemolysis assay *in vitro*

We performed a hemolysis assay to assess the blood compatibility of the developed hydro-films, as it is essential for biomaterials in contact with blood to induce minimal hemolysis, *i.e.*, minimal destruction of red blood cells in response to shear stress or changes in osmotic pressure.[43] The tested hydro-films demonstrated a very low hemolysis rate, measuring lower than 0.02% (0.014 ± 0.008% and 0.018 ± 0.014% for G and GA hydro-films, respectively. Therefore, both G and GA hydro-films were found to be non-hemolytic, as the maximum allowable hemolysis rate for biomaterials is 5%.[44]

Cell culture studies

Cytotoxicity. Even if the biocompatibility of the main components of the hydro-films, such as gelatin, agar, citric acid, AV and EGF,[7,12,41,45,46] has been widely described, it is necessary to determine the cytocompatibility of the complete formulation, to check whether the synergistic action between them could alter their properties, causing cell death.

We assessed the cytocompatibility of the hydro-films in human fibroblasts (HDF cells) and keratinocytes (HaCaT cells), since those are the main cell types present in human skin and have a key role in wound healing.[24] We analyzed cytotoxicity both directly, by placing hydro-films on top of the cells, and indirectly, incubating cells with conditioned media obtained after a 24 h lixiviation of hydro-films. Results given in Fig. 3A and B showed that all the hydro-films were cytocompatible, since cell viability remained above 70% with respect to the untreated control (C−) as stated in the ISO 10993-5 guidelines,

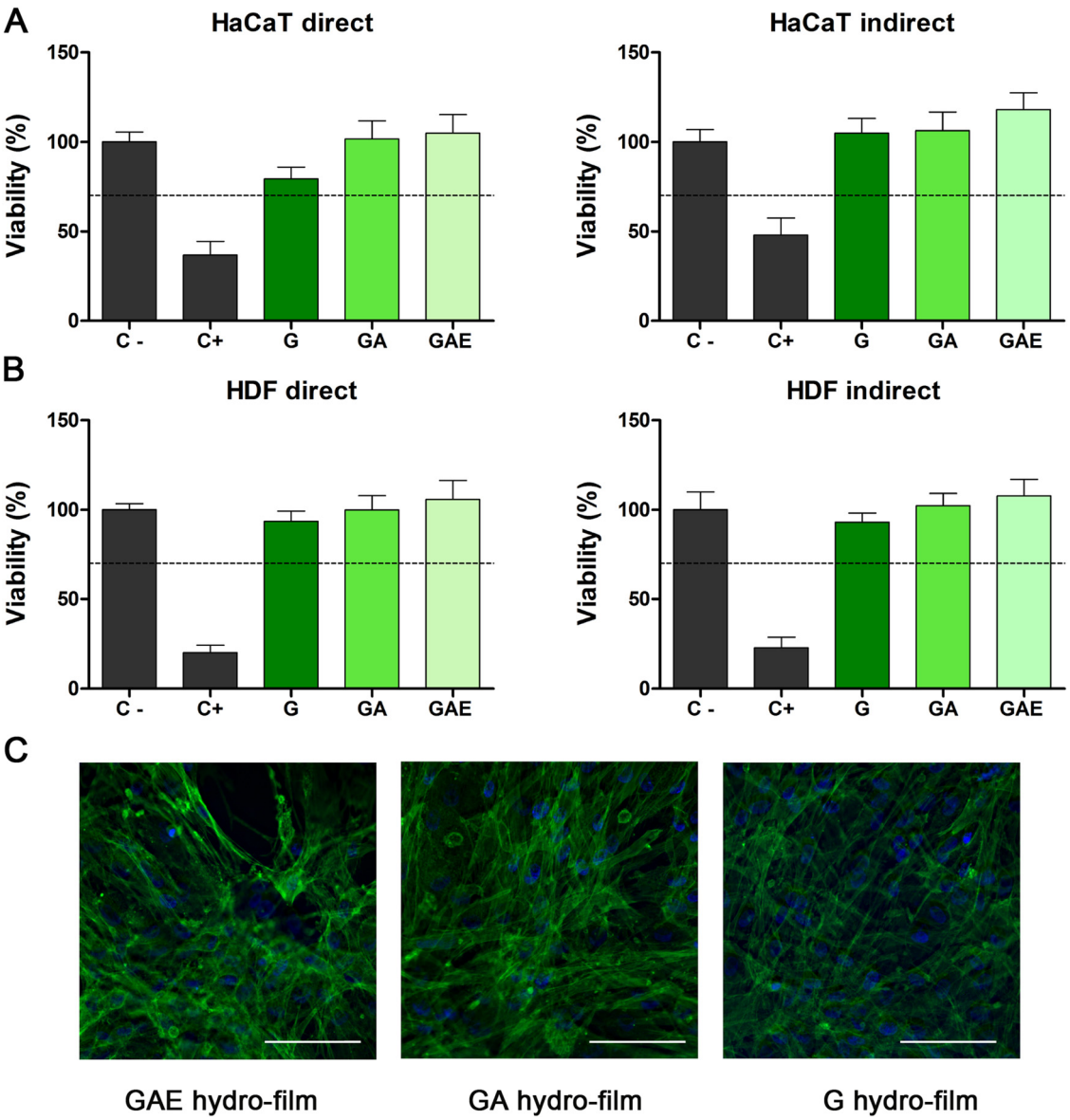

Fig. 3 *In vitro* assays in human cell lines. Cytotoxicity assay on (A) HaCaT and (B) HDF cells, direct and indirect assays. Results are displayed as mean ± SD percentage of viability regarding control. (C) Confocal images of fibroblast adhesion onto the surface of the developed hydro-films. Nuclei are stained in blue and F-actin in green. The scale bars indicates 100 μm.

for all the tested formulations and conditions. Therefore, we obtained cytocompatible hydro-films using the combination of widely described biocompatible components.

Adherence studies. As observed in Fig. 3C fibroblasts were able to adhere on the surface of all the assayed hydro-films – G, GA and GAE hydro-films – showing their typical elongated and spindle-shaped morphology. That excellent fibroblast attachment ability of the hydro-films is of great interest, since it could favor proliferation and tissue remodeling by acting as a provisional matrix where cells can migrate until the development of a new ECM.[47] The cell adhesion was likely. facilitated by the RGD motifs in gelatin, which resembled integrin mediated cell attachment.[16,48,49] It is worth to mention that although AV has shown to enhance cell attachment due to the ability of glucomannan to bind on b2-integrins, we did not observe any differences between G and GA hydro-films[16]

Anti-inflammatory study. To determine the anti-inflammatory activity of the hydro-films, we followed the experimental design represented in Fig. 4A. Briefly, we first differentiated THP-1 human monocytes into macrophages with PMA until they became adherent cells. Then, we incubated cells with conditioned medium of the hydro-films and 2 h later, we added LPS to determine the ability of the hydro-films to prevent the macrophage activation caused by the LPS. For that purpose, we collected cell supernatants and we analyzed the secretion of TNF-α and IL-8, two pro-inflammatory cytokines released by the LPS-activated macrophages.[50] GA and GAE, but not G, hydro-films were able to significantly reduce TNF-α secretion in comparison to cells treated only with LPS (C+), since TNF-α concentrations normalized by cell viability were 2.8 ± 1.1 ng mL^{-1}, 3 ± 0.9 ng mL^{-1}, 3.5 ± 1.3 ng mL^{-1} and 4.8 ± 1.3 ng mL^{-1}, respectively (Fig. 4B). Regarding IL8, all the hydro-film tested were able to decrease its secretion and thus reduce the macrophage activation in comparison to C+ (Fig. 4C). No differences were found between the hydro-films with either cytokine.

One of the most notable features of chronic wounds is their persistent inflammatory state, due to a positive feedback loop that leads to the presence of immune cells throughout all the healing process. Those immune cells are responsible for the release of an excessive amount of matrix metalloproteinases (MMP), creating a proteolytic microenvironment that favors the degradation of the wound matrix and also of the GFs of endogenous or exogenous origin. Therefore, the anti-inflammatory effect exerted by the hydro-films could reduce macrophage activation, thereby reducing that positive feedback loop and helping wounds to progress to a proliferative phase.[24] The anti-inflammatory activity was driven by a combination of the effects of AV and citric acid. Several investigators have reported the anti-inflammatory effect of AV, reducing MMP-9, IL-1β and TNF-α secretion *in vitro*,[51,52] or even reducing the inflammatory infiltration in a wound healing model *in vivo*.[53] These effects have been related to aloe emodin, a compound present in AV.[54] On the other hand, the anti-inflammatory effect of citric acid was displayed *via* the inhibition NF-κB and IRF-3 signaling pathways and the TLR-stimulating signal transduction pathway, as previously described.[55,56]

Scratch assay. We conducted an *in vitro* scratch assay in human keratinocytes and fibroblasts to analyze the effect of the hydro-films in cell migration. We created a gap in a cell monolayer, and we quantified the reduction of the gap area in comparison to the initial area at selected time points.

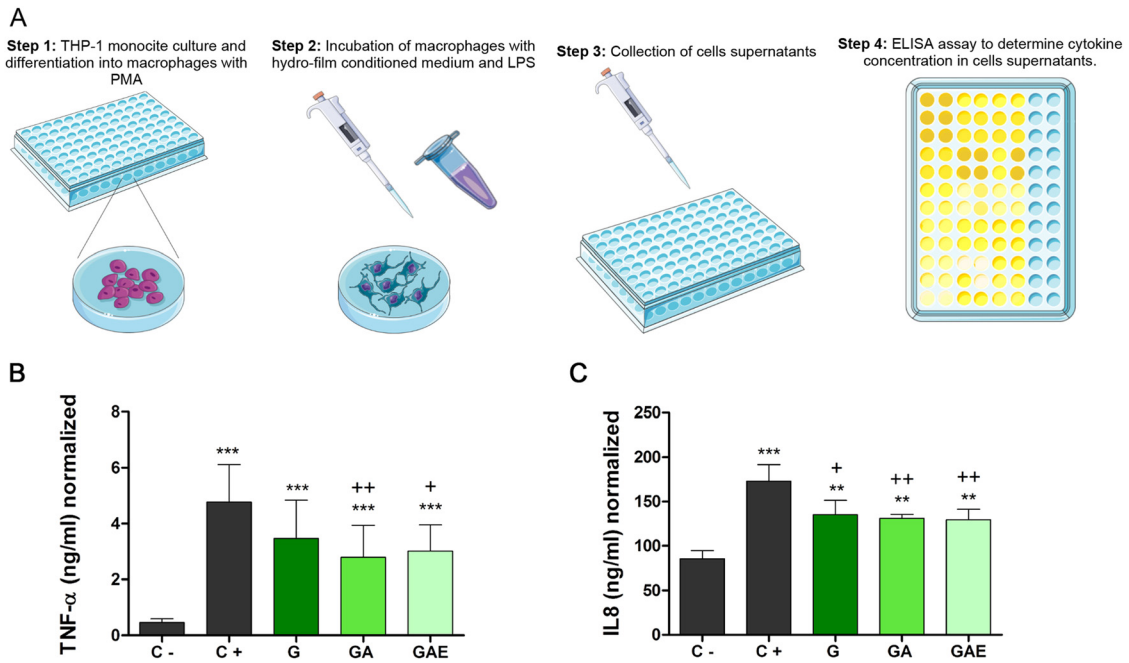

Fig. 4 Anti-inflammatory assay. (A) Experimental design. Results are expressed as the secretion of TNF-α (B) and IL-8 (C), normalized by the viability of each group. ** $p < 0.01$ and *** $p < 0.001$ in comparison to the negative control and +$p < 0.05$ and ++$p < 0.01$ in comparison to the positive control.

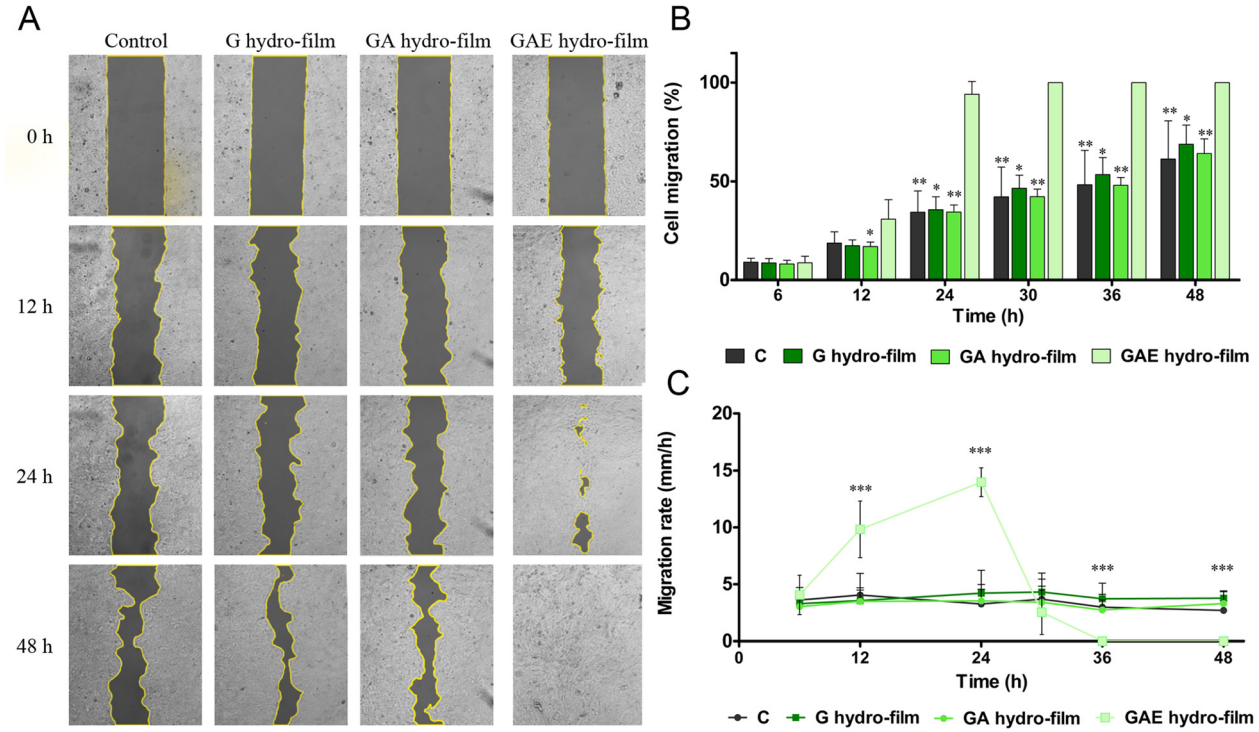

Fig. 5 *In vitro* scratch assay in HaCaT cells. (A) Images of cell migration at different time points. (B) Quantitative analysis of cell migration, results are displayed as mean ± SD percentage of cell migration in regards to the initial gap size. $p < 0.05$, $^{**}p < 0.01$ and $^{***}p < 0.001$ comparing with GAE hydro-films. (C) Migration rate, expressed as cellular progress in function of time. $^{+++}p < 0.001$ comparing GAE hydro-film with the rest of the groups.

Fig. 5 shows the results obtained with keratinocytes. As observed in the representative images of each group (Fig. 5A) and in their graphical representation (Fig. 5B), GAE hydro-films significantly enhanced cell migration from 24 h onwards, in comparison to the rest of the groups. In fact, wounds treated with GAE hydro-films were completely closed at 30 h, while cell migration was less than 50% for the rest of the groups. In particular at 30 h, cell migration achieved values of 42.2 ± 15%, 46.5 ± 6.6% and 42.2 ± 3.9% for untreated group, G hydro-film group and GA hydro-film group, respectively.

Those results were in agreement with the ones obtained in the migration rate analysis (Fig. 5C) since keratinocytes treated with GAE hydro-film presented a faster migration rate at 12 and 24 h compared to the rest of the groups. Migration rate was drastically reduced at 36 h and 48 h in the GAE hydro-film group, since wounds closed completely at 30 h. Regarding, the rest of the groups, we did not find any differences between them in cell migration or migration rate. We attributed the promotion of cell migration to the EGF released from GAE hydro-films, since it promotes keratinocyte migration and proliferation by PI3K-Akt axis activation through EGFR phosphorylation.[24,57] Although we only determined the effect of EGF on cell migration *in vitro*, Ogino *et al.* observed that EGF loaded into gelatin sheets was able to induce reepithelization in a partial thickness wound model conducted in mice.[58] Regarding the effect of AV, its impact in keratinocyte migration was despicable, since GA hydro-films did not improve cell migration in comparison to the control.

Furthermore, we conducted a scratch study in HaCaT cells using mitomycin to ensure that the observed regenerative effect is indeed due to cell migration, as mitomycin inhibits cell proliferation. The results obtained were similar to those achieved using low-serum medium, showing that the GAE hydro-film treatment also accelerated cell migration in this case (Fig. 2). However, with the use of mitomycin, we observed complete gap closure at 24 h and 48 h with G and GA hydro-films. This suggests that the use of low-serum medium may be more restrictive compared to mitomycin in terms of cell migration.

On the other hand, the results obtained with fibroblasts were quite different (Fig. 6A). In this case, both GA and GAE hydro-films significantly enhanced cell migration since the beginning of the study in comparison to the control group (Fig. 6B). They also improved cell migration in comparison to G hydro-films, however that difference was only statistically significant at some time points: with GAE hydro-films at 24 h, 30 h, 36 h and 48 h, and with GA hydro-films at 12 h, 24 h and 48 h. There were no differences among the control group and the G hydro-film group. Therefore, in this case the effect of AV was more noticeable, due to the effect of AV on the promotion of fibroblast migration.[59–61] Shafaie *et al.* suggested that AV could increase the expression of α1β1 integrins, improving wound closure.[59]

We obtained similar results after the analysis of the migration rate (Fig. 6C). GA and GAE hydro-films showed an augmented migration rate in comparison to the control until 30 h. In addition, GAE hydro-films showed a significantly increased

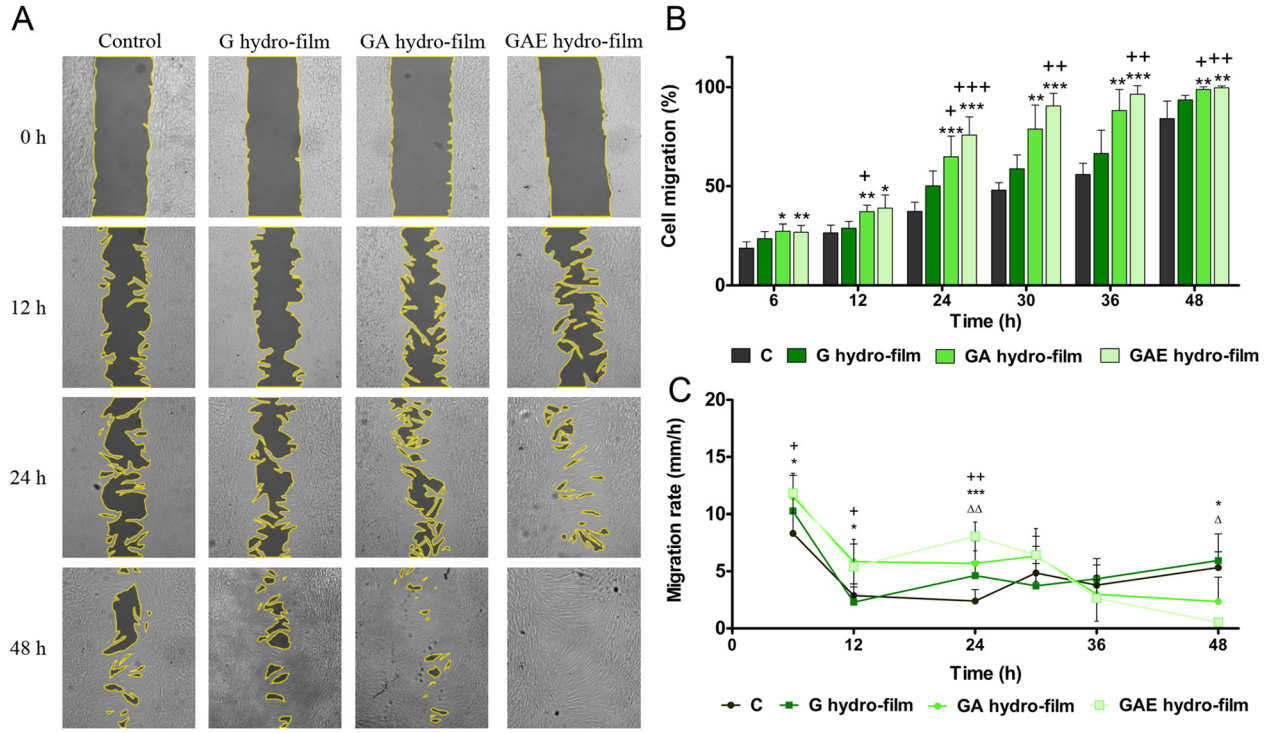

Fig. 6 *In vitro* scratch assay in HDF cells. (A) Images of cell migration at different time points. (B) Quantitative analysis of cell migration, results are displayed as mean ± SD percentage of cell migration in regards to the initial gap size. * $p < 0.05$, ** $p < 0.01$ and *** $p < 0.001$ in comparison to control and + $p < 0.05$, ++ $p < 0.01$ and +++ $p < 0.001$ in comparison to G hydro-film. (C) Migration rate, expressed as cellular progress in function of time. + $p < 0.05$ and ++ $p < 0.01$ comparing C and GA hydro-films, * $p < 0.05$ and *** $p < 0.001$ comparing C and GAE hydro-film, and Δ $p < 0.05$ and ΔΔ $p < 0.01$ comparing G hydro-film and GAE hydro-film.

migration rate in comparison to G hydro-films at 24 h. As observed with the keratinocytes, from 36 h onwards the migration rate obtained with GA and GAE hydro-films decreased, since wounds were almost closed by then.

Overall, we have developed agar/gelatin hydro-films for chronic wound healing cross-linked with citric acid, containing the active compounds AV and EGF, the first one as a structural part of the matrix and the second one absorbed on the nanopores of the matrix due to electrostatic interactions. Notably, this is the first time that AV and EGF have been combined in agar/gelatin hydro-films for wound healing applications. While similar component combinations have been explored in other studies, such as AV and EGF in nanofibers[15] or gelatin/hyaluronic acid scaffolds,[62] our approach tries to overcome some of the challenges associated with these materials by leveraging the unique properties of all the components in a synergistic manner.

In this context, we have successfully addressed the weak mechanical properties of gelatin by incorporating agar and using citric acid as a non-toxic cross-linker, avoiding the use of aldehydes. Moreover, the combination of EGF, AV, and citric acid in our hydro-films has been shown to enhance wound healing through complementary mechanisms, including promoting and migration of keratinocytes and fibroblasts, as well as exhibiting anti-inflammatory activity, which are, key aspect of the chronicity of wounds. As a result, our hydro-films possess unique characteristics that make them highly suitable for wound healing applications, including their composition of inexpensive and biocompatible materials, favorable mechanical properties for easy handling and application, transparency for wound monitoring, precise control of wound moisture, and promotion of wound healing through complementary mechanisms. By addressing multiple aspects of chronic wounds, our hydro-films represent an innovative approach with the potential to significantly improve wound healing outcomes.

Experimental

Hydro-film preparation

Porcine gelatin (type A, 250 bloom) was purchased from Sancho de Borja (Borja, Spain), agar (4.63 g SO_4^{2-} per kg) was provided by Hai Long Robika Factory (Dong Thap, Vietnam), and AV powder by Agora Valencia (Valencia, Spain). Glycerol (purity of 99.01%), used as plasticizer, and anhydrous citric acid, used as cross-linker, were obtained from Panreac (Barcelona, Spain). All chemicals were of food grade and they were used as received without further purification.

Three types of hydro-films were produced by solution casting, G hydro-films, GA hydro-films and GAE hydro-films (Table 1). To produce G hydro-films, 5 g of porcine gelatin were mixed with citric acid (20 wt% on a gelatin basis) in 60 mL of milliQ water at

Table 1 Components of G, GA and GAE hydro-films

G hydro-film	GA hydro-film	GAE hydro-film
55.6% Porcine gelatin	50% Porcine gelatin	50% Porcine gelatin
11.1% Citric acid	10% Citric acid	10% Citric acid
22.2% Agar	20% Agar	20% Agar
11.1% Glycerol	10% Glycerol	10% Glycerol
	10% AV powder	10% AV powder
		0,1% EGF

80 °C and 200 rpm for 30 min. In the meanwhile, agar (40 wt% on a gelatin basis) was dissolved in 40 mL of distilled water at 105 °C and 200 rpm for 30 min. Then, these two solutions were mixed, and 20 wt% glycerol (on a gelatin basis) was added. The solution pH was adjusted to 10 with NaOH (1 M) and it was heated at 80 °C and 200 rpm for 30 min. Finally, the solution was poured into Petri dishes and left to dry for 48 h at room temperature to obtain G hydro-films. GA hydro films were produced following the same method, the only difference being the addition of 20 wt% AV (on a gelatin basis) to the gelatin solution with citric acid. Hydro-films were cut into discs of different diameters, according to the type of experiment to be performed, using a punch (3–20 mm, JLB320CM, Boehm, France). GAE hydro-films were prepared adding a 0.5 mg mL^{-1} EGF solution (Miltenyi Biotech, Germany) dropwise onto GA hydro-film discs, and they were left overnight to allow water evaporation and EGF absorption. A diagram of the hydro-films preparation is depicted in Fig. 7.

Hydro-film characterization.

Fourier transform infrared (FTIR) spectroscopy. FTIR spectra of G and GA hydro-films were recorded by a Platinum-ATR Alpha II FTIR spectrometer (Bruker). A total of 32 scans were performed at 4 cm^{-1} resolution. Measurements were recorded between 4000 and 800 cm^{-1}.

X-Ray diffraction (XRD). XRD patterns of G and GA hydro-films were analyzed using a diffraction unit (PANalytic Xpert PRO). These analyses were run with Cu-Kα (λ = 1.5418 Å) radiation at current of 40 mA and voltage of 40 kV. Samples were scanned between $2\theta = 2^\circ$ to 50°, θ being the incidence angle of the X-ray beam on the sample.

Scanning electron microscopy (SEM). S-4800 field emission scanning electron microscope (Hitachi High-Technologies Corporation) was employed to visualize the hydro-films inner and surface morphologies. Prior to observation, samples were mounted on a metal stub with a double-side adhesive tape and coated under vacuum with gold using a JEOL fine-coat ion sputter (JFC-1100) in argon atmosphere. The accelerating voltage used during image acquisition was 5 kV.

Water uptake (WU). Water uptake was determined following the same procedure used in previous studies of our research group.[11] To determine the water uptake curve, dry samples of G and GA hydro-films were cut into discs of 8 mm in diameter.

Then, discs were weighed and immersed into 1 mL of PBS at 37 °C (pH 7.4, Gibco® Life technologies, USA). The hydro-films were collected at selected time points (5 min, 30 min, 1 h, 2 h 4 h, 8 h and 24 h), the excess of water was removed, and their wet weight was determined. The percentage of water uptake (WU) was calculated using the following equation (eqn (1)):

$$\mathrm{WU}(\%) = \frac{W - W_0}{W_0} \times 100 \quad (1)$$

where W is the weight of the wet hydro-film at each time point and W_0 is the initial dry weight.

Following the same procedure, the effect of pH in the hydro-film swelling was also analyzed. For that, instead of immersing the hydro-films into PBS, they were immersed in pH 5 and pH 8 buffers, to simulate the pH of the skin and of the wounds, respectively. This study was carried out up to 72 h.

Hydrolytic degradation. G and GA hydro-film discs of 8 mm in diameter were weighed and maintained in PBS at 37 °C until various time points (0 h, 1 h, 4 h, 8 h, 24 h, 4 days, 7 days, 14 days, 21 days and 28 days). At those selected points, discs were collected, washed with MilliQ water and freeze-dried. Finally, the lyophilized discs were weighed and the percentage of the remaining weight (RW) was calculated through the

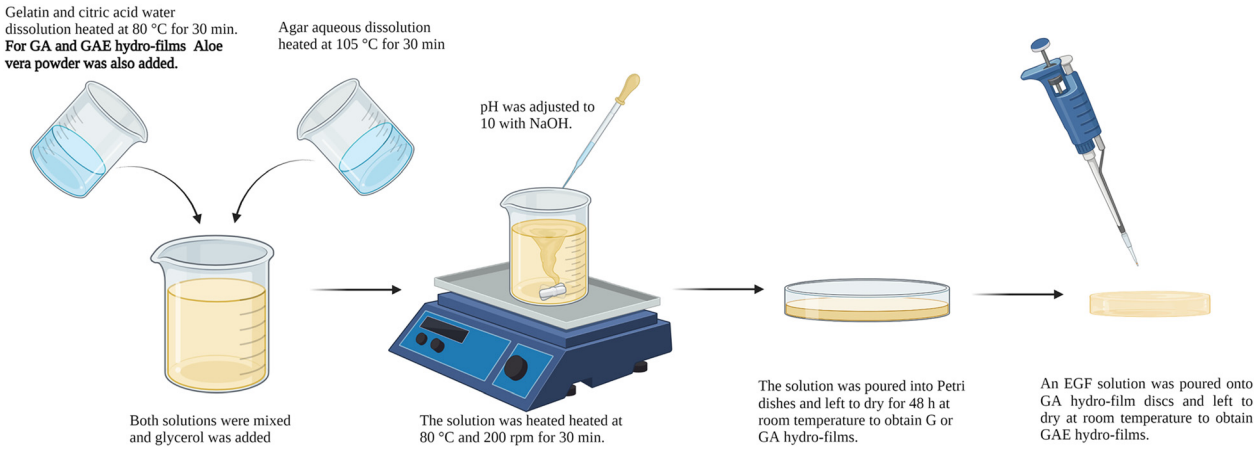

Fig. 7 Diagram of the G, GA and GAE hydro-film preparation.

following equation (eqn (2)):

$$\mathrm{RW}(\%) = \frac{\text{Dry weight at time points}}{\text{Dry weight at time 0}} \times 100 \quad (2)$$

To analyze the effect of pH in the degradation of the hydro-films, buffers with pH 5 and pH 8 were used instead of PBS, to simulate the pH of native skin and of wounded skin, respectively. The study was conducted for 72 h.

Mechanical properties. Tensile strength (TS) and elongation at break (EB) of hydro-films were determined using Insight 10 Electromechanical Testing System (MTS Systems) and following ASTM D638-03 method (ASTM, 2003). The tensile test was conducted with a load cell of 250 N and a fixed crosshead speed of 1 mm min^{-1}. Dog bone shape sample with 22.25 mm length and 4.75 mm width was used. All samples were conditioned at 100% relative humidity and 23 °C for 48 h prior to testing. For each formulation, 5 samples were tested and average values were reported.

Water vapor transmission rate (WVTR). WVTR was determined in a controlled humidity environment chamber PERME™ W3/0120 (Labthink Instruments Co. Ltd), according to ASTM E96-00 (ASTM, 2000). G and GA hydro-film discs (ϕ = 7.40 cm) were cut and sealed to cups containing distilled water. The setup was subjected to a temperature of 38 °C and a relative humidity of 90%. Water vapor transmission rate (WVTR) was calculated by the following equation (eqn (3)):

$$\mathrm{WVTR}\left(\frac{g}{s \cdot \mathrm{cm}^2}\right) = \frac{G}{t \cdot A} \quad (3)$$

where G is the change in weight (g), t is time (s), and A is the test area (cm^2), which corresponded to 33 cm^2.

Contact angle. Water contact angle measurements were performed using an OCA 20 contact angle system (DataPhysics Instruments). A 3 μL droplet of distilled water was placed on film surface to estimate the hydrophobic character and the image of the drop was carried out using SCA20 software. Measurements were performed for each composition at 23 °C at the time of drop deposition and 5 min after drop deposition.

EGF release profile. To study the release of EGF, GAE hydro-film discs of 8 mm in diameter were used. The discs were transferred to ultra-low attachment 24 well plates (Corning, NY, USA) containing 1 mL of PBS. The discs were incubated at 37 °C and, at selected time points, the medium was collected and replaced with fresh PBS. EGF concentration on the collected PBS was quantified using a commercial ELISA kit for human EGF (Quantikine, R & D Systems, MN, USA) following the manufacturers' instructions. The results were expressed as the released percentage of the total EGF content in the discs.

Hemolysis assay *in vitro*. Blood was obtained from healthy volunteers in accordance with the protocols approved by the Ethics Committee for Research Involving Human Beings of the University of the Basque Country (Procedure number: M10/2021/256) and the Ethics Committee for Research Involving Biological Agents & GMOs (Procedure number: M30/2021/257). For hemocompatibility assessment *in vitro*, citrated whole blood (in a 9 : 1 ratio of whole blood to 3.8% sodium citrate) was obtained from a healthy donor and diluted 1 : 5 in normal saline. G and GA hydro-film discs of 8 mm were placed in a 24 well plate. 200 μL of diluted whole blood was added to each sample, and the plate was incubated for 1 h at 37 °C. Then, the hydro-films and blood were centrifuged for 10 minutes at 3000 rpm. The serum supernatants were collected, and their hemoglobin content was quantified using a commercial kit (Hemoglobin Assay Kit, Sigma-Aldrich, USA) following the manufacturer's instructions. Whole blood diluted 1 : 5 with deionized water (C+) was used as the positive control, and whole blood diluted 1 : 5 with normal saline (C−) was used as the negative control. The hemolysis rate was calculated using the following equation, where HF is the hydro-film's hemoglobin content, and C(−) and C(+) negative and positive control's hemoglobin content, respectively (eqn (4)):

$$\mathrm{Hemolysis}(\%) = \frac{\mathrm{HF} - \mathrm{C}(-)}{\mathrm{C}(+) - \mathrm{C}(-)} \times 100 \quad (4)$$

In vitro cell culture studies in human cells

Cell culture. In the current study, three human cell lines were used: HaCaT keratinocytes, primary human dermal fibroblasts isolated from adult skin (HDFs), and THP-1 monocytes. HaCaT cells (DKFZ, Germany) were cultured on Dulbecco's modified Eagle's medium (DMEM) (41965-039, Gibco®, MA, USA) supplemented with 10% (v/v) foetal bovine serum (FBS) and 1% (v/v) penicillin-streptomycin.[63] HDF cells (ATCC®, VA, USA) were cultured on their complete medium that consist on fibroblast basal medium (PCS-201-030, ATCC®, VA, USA) supplemented with fibroblast growth kit-low serum (PCS-201-041, ATCC®, VA, USA) and 1% (v/v) penicillin-streptomycin. THP-1 monocytes (ATCC®, VA, USA) were cultured on RPMI-1640 medium (30-2001 ATCC®, VA, USA) supplemented with 10% (v/v) FBS and 1% (v/v) penicillin-streptomycin. Cell lines were incubated in a humidified incubator with a 5% CO_2 atmosphere at 37 °C and cell passages or medium changes were performed every 3–6 days depending on the cell line.

Cell viability studies. Hydro-film biocompatibility was assessed in HDF and HaCaT cells, determining direct and indirect cytotoxicity, following the ISO 10993-5 guideline. Direct cytotoxicity was measured placing the hydro-films on top of the cells and incubating them for 48 h. Indirect cytotoxicity, on the other way, was quantified incubating cells with conditioned media obtained after lixiviating the hydro-films, also for 48 h.

For direct cytotoxicity studies, HDF cells were seeded at a density of 35 000 cells per well and HaCaT cells at a density of 70 000 cells per well on 24 well plates, and were incubated overnight to ensure cell adhesion. Then, G, GA or GAE hydro-films discs of 8 mm in diameter were added to the wells. Culture medium with 10% (v/v) DMSO and fresh culture medium were used as positive and negative controls, respectively. After incubating the cells with the discs for 48 h, cell viability was determined using a CCK-8 colorimetric assay (Cell Counting Kit-8, Sigma-Aldrich, MO, USA). For the assay, the hydro-film discs were removed from the wells, 10 μL of the CCK-8 reagent were added to the wells and cells were incubated

for 4 h. Then, their absorbance was measured at 450 nm, using 650 nm as reference wavelength (Plate Reader Infinite M200, Tecan, Switzerland). The obtained value in each well was directly proportional to the number of living cells in them. Results were expressed as the percentage of cell viability compared to the control.

For indirect cytotoxicity studies, firstly, the conditioned medium of the hydro-films was obtained by lixiviation. For that, hydro-film discs of 8 mm in diameter were incubated with 0.5 mL of culture medium for 24 h at 37 °C. In addition, 0.5 mL of culture medium and 0.5 mL of culture medium with 10% (v/v) DMSO were also incubated to be used as negative and positive controls, respectively.

Meanwhile, HDF cells were seeded at a density of 5000 cells per well and HaCaT cells at a density of 10 000 cells per wells in a 96 well plate. After an overnight incubation, the culture medium was replaced by the conditioned medium of the hydro-films and the controls. Then, cells were incubated for 48 h with the conditioned medium and finally cell viability was measured through the CCK-8 colorimetric assay as in the direct cytotoxicity assay.

Cell adhesion assay. G, GA and GAE hydro-film discs of 8 mm in diameter were placed in ultra low attachment plates of 24 wells (Corning, NY, USA). On top of each hydro-film disc, 25 000 HDF cells were seeded in culture medium without FBS. After a 6 h incubation that allowed cells to adhere, the culture medium was changed by complete medium, and cells were let to spread overnight. Then, hydro-films were fixed with 3.7% formaldehyde (Panreac, Spain); membranes were permeabilized with Triton-X (Sigma-Aldrich, MO, USA), and the cells were stained with Alexa Fluor 488-labelled Phalloidin for F-actin (Thermo Fisher Scientific, MA, USA) and with DAPI for the nuclei (Thermo Fisher Scientific, MA, USA) following the manufacturer's instructions. Fluorescent micrographs were acquired using a confocal fluorescence microscope (Nikon epi-fluorescence microscope equipped with a DSD2 confocal Modulus, Nikon, Japan).

Anti-inflammatory assay. The anti-inflammatory assay was conducted following the procedure described by Zhao *et al.*[64] with slights modifications. THP-1 human monocytes were seeded at a density of 500 000 cell mL^{-1} in 96 well plates and phorbol miristate (PMA) (Abcam, UK) was added to a final concentration of 30 ng mL^{-1} to allow monocyte differentiation into macrophages. After 48 of incubation, culture medium was replaced with conditioned medium obtained in the same conditions as in cell viability studies section. Cells were incubated for 2 h and then, lipopolysaccharide (LPS) (Sigma-Aldrich, MO, USA) was added to a final concentration of 100 ng mL^{-1}. Plain culture medium was used as negative control, and culture medium with 100 ng mL^{-1} of LPS as positive control. Cell supernatants were collected after 24 h to quantify IL-8 and TNF-α concentration, using commercially available ELISA kits (Prepotech, NJ, USA and Biolegend, CA, USA, respectively).

In addition, cell viability was determined through a CCK-8 colorimetric assay, following the same procedure as in cell viability studies section, to normalize the cytokine concentration. Therefore, results were given as the secreted IL-8 and TNF-α concentration normalized by cell viability in each group.

***In vitro* wound healing assay.** For this study, we followed a modified procedure of the one described by Chiu *et al.*[65] Firstly, Ibidis 2 well culture inserts (Ibidi, Germany) were placed on 6 well plates and either HDF or HaCaT cells were seeded at a density of 500 000 cell mL^{-1} onto them. After incubating cells for 6 h, they were put under starving conditions, *i.e.* the HDF cells medium was changed by serum free medium and the HaCaT cells medium by medium with 167% (v/v) of FBS. Cells were incubated in those conditions overnight, to allow the formation of a cell monolayer, and then culture inserts were removed using sterile tweezers, creating a cell gap of 500 μm. Subsequently, G, GA or GAE hydro-films were added to the wells and the cell gap closure was monitored under an inverted phase microscope (Eclipse TE2000-S, Nikon, Japan), taking micrographs at selected time points: 0 h, 6 h, 12 h, 24 h, 30 h, 36 h and 48 h.

Furthermore, a cell migration assay was performed using mitomycin to inhibit cell proliferation. The HaCaT cell line was utilized, and a similar protocol as the previous assay was followed with minor modifications. Prior to removing the culture inserts, cells were treated with mitomycin at a concentration of 5 mg mL^{-1} for a 2-hour incubation period. Subsequently, the mitomycin-containing medium was removed and replaced with complete medium. Finally, the inserts were removed, and the assay was conducted following the same procedure as in the previous case.

Statistical analysis. We performed each experiment in triplicate and in three independent assays. The results were expressed as the mean ± standard deviation (SD). When the results showed a normal distribution following the Shapiro-Wilks normality test, they were analyzed using the Student's *t*-test for two independent samples or ANOVA test for multiple comparison. In the ANOVA test, Bonferroni or Tamhane *post hoc* were applied, based on the Levene test for the homogeneity of variances. When the results did not show a normal distribution, Mann Whitneys U test for two samples or Kruskal Wallis test for multiple comparison were performed. SPSS 22.0.01 (SPSS®, INC., IL, USA) was used for the statistical analysis and the graphs were created using GraphPad Prism (v.5.01, GraphPad Software, Inc, USA).

Conclusions

In the current study, we prepared hydro-films composed of gelatin, agar and AV, which were cross-linked with citric acid. The cross-linking reaction that was confirmed by the FTIR and XRD spectra, led to easy to handle hydro-films, with a slow degradation rate, since after 28 days in PBS at 37 °C, 28 ± 8% of the initial weight remained. Then, we added EGF dropwise onto GA hydro-films to obtain GAE hydro-films that release EGF in a biphasic way, with an initial burst release that lasted 2 h and a slower phase until the complete EGF release at 48 h. These hydro-films showed an appropriate moisture control for wound

healing, since they were able to absorb water up to 900% of their dry weight, which may help absorb the excess of exudate. In addition, their WVTR was suited to maintain a balance between excessive moisture, which can lead to wound maceration, and a dry, painful wound. Their ultimate tensile strength was in the highest range of that of human skin (31 ± 2 MPa), revealing the adequate mechanical properties of the developed hydro-films.

Regarding the wound healing efficacy of hydro-films, we observed that they presented a synergistic activity for the treatment of chronic wounds. They were able to reduce macrophage activation in comparison to the control and, thus, we hypothesize that they would be able to reduce the excessive inflammatory response of chronic wounds. In addition, they promoted cell migration in both keratinocytes and fibroblasts, which is a crucial step to achieve wound closure. Moreover, cells were able to adhere to hydro-films, so they could act as provisional matrices for cells to migrate until the development of a new ECM. Accordingly, the results indicate that our innovative approach represents a promising advancement in the development of wound dressings with superior performance.

Author contributions

Itxaso Garcia-Orue: conceptualization, methodology, formal analysis, investigation, resources, writing-original draft, visualization. Edorta Santos-Vizcaino: conceptualization, methodology, writing-review & editing, supervision, project administration. Jone Uranga: investigation, writing-review & editing. Koro de la Caba: conceptualization, writing-review & editing, supervision. Pedro Guerrero: conceptualization, methodology, writing-review & editing, supervision. Manoli Igartua: conceptualization, writing-review & editing, supervision, project administration, funding acquisition. Rosa Maria Hernandez: conceptualization, writing-review & editing, supervision, project administration, funding acquisition.

Conflicts of interest

There are no conflicts to declare.

Acknowledgements

This work has been partially supported by the Basque Government (Consolidated Groups, IT1448-22 and IT1658-22) and by PID2021-124294OB-C22 project funded by MCIN/AEI/10.13039/501100011033/FEDER, UE. The authors are thankful for the technical and human support provided by SGIker of UPV/EHU and European funding (ERDF and ESF). Authors also thank ICTS ''NANBIOSIS'', specifically the Drug Formulation Unit (U10) of the CIBER in Bioengineering, Biomaterials and Nanomedicine (CIBER-BBN) at the University of Basque Country UPV/EHU in Vitoria-Gasteiz. J. U. thanks the UPV/EHU for her fellowship (ESPDOC21/74). Biorended was used to create the graphical abstract and Fig. 4.

Notes and references

1 S. R. Nussbaum, M. J. Carter, C. E. Fife, J. DaVanzo, R. Haught, M. Nusgart and D. Cartwright, *Value Health.*, 2018, **21**, 27–32.
2 G. Han and R. Ceilley, *Adv. Ther.*, 2017, **34**, 599–610, DOI: **10.1007/s12325-017-0478-y**.
3 C. Lindholm and R. Searle, *Int. Wound J.*, 2016, **13**, 5–15, DOI: **10.1111/iwj.12623**.
4 A. Gaspar-Pintiliescu, A. M. Stanciuc and O. Craciunescu, *Int. J. Biol. Macromol.*, 2019, **138**, 854–865.
5 J. I. Kang and K. M. Park, *J. Mater. Chem. B*, 2021, **9**, 1503–1520, DOI: **10.1039/d0tb02582h**.
6 S. P. Ndlovu, K. Ngece, S. Alven and B. A. Aderibigbe, *Polymers*, 2021, **13**(17), 2959, DOI: **10.3390/polym13172959**.
7 R. Naomi, H. Bahari, P. M. Ridzuan and F. Othman, *Polymers*, 2021, **13**(14), 2319, DOI: **10.3390/polym13142319**.
8 A. L. Martinez-Lopez, C. Pangua, C. Reboredo, R. Campion, J. Morales-Gracia and J. M. Irache, *Int. J. Pharm.*, 2020, **581**, 119289.
9 A. Francesko, P. Petkova and T. Tzanov, *Curr. Med. Chem.*, 2018, **25**, 5782–5797, DOI: **10.2174/0929867324666170920161246**.
10 L. I. Moura, A. M. Dias, E. Carvalho and H. C. de Sousa, *Acta Biomater.*, 2013, **9**, 7093–7114, DOI: **10.1016/j.actbio.2013.03.033**.
11 I. Garcia-Orue, E. Santos-Vizcaino, A. Etxabide, J. Uranga, A. Bayat, P. Guerrero, M. Igartua, K. de la Caba and R. M. Hernandez, *Pharmaceutics*, 2019, **11**, 314, DOI: **10.3390/pharmaceutics11070314**.
12 S. Shen, X. Chen, Z. Shen and H. Chen, *Pharmaceutics*, 2021, **13**(10), 1666, DOI: **10.3390/pharmaceutics13101666**.
13 S. A. Hashemi, S. A. Madani and S. Abediankenari, *BioMed Res. Int.*, 2015, **2015**, 714216, DOI: **10.1155/2015/714216**.
14 M. Sanchez, E. Gonzalez-Burgos, I. Iglesias and M. P. Gomez-Serranillos, *Molecules*, 2020, **25**(6), 1324, DOI: **10.3390/molecules25061324**.
15 I. Garcia-Orue, G. Gainza, P. Garcia-Garcia, F. B. Gutierrez, J. J. Aguirre, R. M. Hernandez, A. Delgado and M. Igartua, *Int. J. Pharm.*, 2019, **556**, 320–329, DOI: **10.1016/j.ijpharm.2018.12.010**.
16 S. Baghersad, S. Hajir Bahrami, M. R. Mohammadi, M. R. M. Mojtahedi and P. B. Milan, *Mater. Sci. Eng. C. Mater. Biol. Appl.*, 2018, **93**, 367–379.
17 F. Ashouri, F. Beyranvand, N. Beigi Boroujeni, M. Tavafi, A. Sheikhian, A. M. Varzi and S. Shahrokhi, *Drug Deliv. Transl. Res.*, 2019, **9**, 1027–1042, DOI: **10.1007/s13346-019-00643-0**.
18 N. Zhang, T. Gao, Y. Wang, J. Liu, J. Zhang, R. Yao and F. Wu, *Int. J. Biol. Macromol.*, 2020, **154**, 835–843.
19 S. Singh, A. Gupta and B. Gupta, *Int. J. Biol. Macromol.*, 2018, **120**, 1581–1590.
20 L. F. Gomez Chabala, C. E. E. Cuartas and M. E. L. Lopez, *Mar. Drugs*, 2017, **15**(10), 328, DOI: **10.3390/md15100328**.
21 I. Rubio-Elizalde, J. Bernaldez-Sarabia, A. Moreno-Ulloa, C. Vilanova, P. Juarez, A. Licea-Navarro and A. B. Castro-Cesena, *Carbohydr. Polym.*, 2019, **206**, 455–467.

22 A. Sathiyaseelan, A. Shajahan, P. T. Kalaichelvan and V. Kaviyarasan, *Int. J. Biol. Macromol.*, 2017, **104**, 1905–1915.
23 M. Tummalapalli, M. Berthet, B. Verrier, B. L. Deopura, M. S. Alam and B. Gupta, *Int. J. Biol. Macromol.*, 2016, **82**, 104–113, DOI: **10.1016/j.ijbiomac.2015.10.087**.
24 I. Garcia-Orue, J. L. Pedraz, R. M. Hernandez and M. Igartua, *J. Drug Deliv. Sci. Technol.*, 2017, **42**, 2–17, DOI: **10.1016/j.jddst.2017.03.002**.
25 S. Barrientos, H. Brem, O. Stojadinovic and M. Tomic-Canic, *Wound Repair Regen.*, 2014, **22**, 569–578, DOI: **10.1111/wrr.12205**.
26 S. Ogino, N. Morimoto, M. Sakamoto, C. Jinno, T. Taira and S. Suzuki, *J. Surg. Res.*, 2016, **201**, 446–454, DOI: **10.1016/j.jss.2015.11.027**.
27 K. Hori, C. Sotozono, J. Hamuro, K. Yamasaki, Y. Kimura, M. Ozeki, Y. Tabata and S. Kinoshita, *J. Controlled Release*, 2007, **118**, 169–176, DOI: **10.1016/j.jconrel.2006.12.011**.
28 E. K. Tiaka, N. Papanas, A. C. Manolakis and G. S. Georgiadis, *Perspect Vasc Surg Endovasc Ther*, 2012, **24**, 37–44.
29 C. Alemdaroğlu, Z. Degim, N. Celebi, M. Şengezer, M. Alömeroglu and A. Nacar, *J. Biomed. Mater. Res. A*, 2008, **85A**, 271–283, DOI: **10.1002/jbm.a.31588**.
30 L. Diaz-Gomez, I. Gonzalez-Prada, R. Millan, A. Da Silva-Candal, A. Bugallo-Casal, F. Campos, A. Concheiro and C. Alvarez-Lorenzo, *Carbohydr. Polym.*, 2022, **278**, 118924, DOI: **10.1016/j.carbpol.2021.118924**.
31 J. Uranga, I. Leceta, A. Etxabide, P. Guerrero and K. de la Caba, *Eur. Polym. J.*, 2016, **78**, 82–90, DOI: **10.1016/j.eurpolymj.2016.03.017**.
32 N. Yu, J. Li, F. Ma, P. Yang, W. Liu, M. Zhou, Z. Zhu and S. Xing, *J. Agric. Food Chem.*, 2020, **68**, 9537–9545, DOI: **10.1021/acs.jafc.0c01131**.
33 G. U. Rani, A. K. Konreddy and S. Mishra, *Int. J. Biol. Macromol.*, 2018, **117**, 902–910, DOI: **10.1016/j.ijbiomac.2018.05.163**.
34 X. Huang, Q. Fu, Y. Deng, F. Wang, B. Xia, Z. Chen and G. Chen, *Carbohydr. Polym.*, 2021, **253**, 117256, DOI: **10.1016/j.carbpol.2020.117256**.
35 R. F. Pereira, A. Carvalho, M. H. Gil, A. Mendes and P. J. Bártolo, *Carbohydr. Polym.*, 2013, **98**, 311–320, DOI: **10.1016/j.carbpol.2013.05.076**.
36 R. Xu, H. Xia, W. He, Z. Li, J. Zhao, B. Liu, Y. Wang, Q. Lei, Y. Kong, Y. Bai, Z. Yao, R. Yan, H. Li, R. Zhan, S. Yang, G. Luo and J. Wu, *Sci. Rep.*, 2016, **6**, 24596, DOI: **10.1038/srep24596**.
37 M. Rezvanian, N. Ahmad, M. Amin, M. Cairul Iqbal and S. Ng, *Int. J. Biol. Macromol.*, 2017, **97**, 131–140, DOI: **10.1016/j.ijbiomac.2016.12.079**.
38 P. Hubner, N. R. Marcilio and I. C. Tessaro, *J. Biomater. Appl.*, 2021, **36**, 682–700, DOI: **10.1177/0885328221992260**.
39 S. Chen, B. Liu, M. A. Carlson, A. F. Gombart, D. A. Reilly and J. Xie, *Nanomedicine*, 2017, **12**, 1335–1352, DOI: **10.2217/nnm-2017-0017**.
40 J. T. Sánchez, A. V. García, A. Martínez-Abad, F. Vilaplana, A. Jiménez and M. C. Garrigós, *Foods*, 2020, **9**(9), 1248, DOI: **10.3390/foods9091248**.
41 I. Garcia-Orue, G. Gainza, F. B. Gutierrez, J. J. Aguirre, C. Evora, J. L. Pedraz, R. M. Hernandez, A. Delgado and M. Igartua, *Int. J. Pharm.*, 2016, **53**, 556–566, DOI: **10.1016/j.ijpharm.2016.11.006**.
42 A. Etxabide, C. Vairo, E. Santos-Vizcaino, P. Guerrero, J. L. Pedraz, M. Igartua, K. de la Caba and R. M. Hernandez, *Int. J. Pharm.*, 2017, **530**, 455–467, DOI: **10.1016/j.ijpharm.2017.08.001**.
43 M. Weber, H. Steinle, S. Golombek, L. Hann, C. Schlensak, H. P. Wendel and M. Avci-Adali, *Front. Bioeng. Biotechnol.*, 2018, **6**, 99, DOI: **10.3389/fbioe.2018.00099**.
44 J. Zhu, H. Han, F. Li, X. Wang, J. Yu, X. Qin and D. Wu, *Chem. Mater.*, 2019, **31**, 4436–4450, DOI: **10.1021/acs.chemmater.9b00850**.
45 S. Kudłacik-Kramarczyk, A. Drabczyk, M. Głąb, D. Alves-Lima, H. Lin, T. E. L. Douglas, S. Kuciel, A. Zagórska and B. Tyliszczak, *Mater. Sci. Eng., C*, 2021, **123**, 111977, DOI: **10.1016/j.msec.2021.111977**.
46 M. Lambros, T. H. Tran, Q. Fei and M. Nicolaou, *Pharmaceutics*, 2022, **14**(5), 972, DOI: **10.3390/pharmaceutics14050972**.
47 I. Firlar, M. Altunbek, C. McCarthy, M. Ramalingam and G. Camci-Unal, *Gels*, 2022, **8**(2), 127, DOI: **10.3390/gels8020127**.
48 C. Romo-Valera, P. Guerrero, J. Arluzea, J. Etxebarria, K. de la Caba and N. Andollo, *Int. J. Mol. Sci.*, 2021, **22**(7), 3648, DOI: **10.3390/ijms22073648**.
49 C. Torsahakul, N. Israsena, S. Khramchantuk, J. Ratanavaraporn, S. Dhitavat, W. Rodprasert, S. Nantavisai and C. Sawangmake, *PLoS One*, 2022, **17**(2), e0263141, DOI: **10.1371/journal.pone.0263141**.
50 A. Banete, J. Barilo, R. Whittaker and S. Basta, *Front. Microbiol.*, 2022, **12**, 803427, DOI: **10.3389/fmicb.2021.803427**.
51 D. Vijayalakshmi, R. Dhandapani, S. Jayaveni, P. S. Jithendra, C. Rose and A. B. Mandal, *J. Ethnopharmacol.*, 2012, **141**, 542–546, DOI: **10.1016/j.jep.2012.02.040**.
52 B. Bhar, B. Chakraborty, S. K. Nandi and B. B. Mandal, *Int. J. Biol. Macromol.*, 2022, **203**, 623–637, DOI: **10.1016/j.ijbiomac.2022.01.142**.
53 A. Y. Koga, J. C. Felix, R. G. M. Silvestre, L. C. Lipinski, B. Carletto, F. A. Kawahara and A. V. Pereira, *Acta Cir Bras*, 2020, **35**, e202000507, DOI: **10.1590/s0102-86502020005 0000007**.
54 B. Gorain, M. Pandey, N. H. Leng, C. W. Yan, K. W. Nie, S. J. Kaur, V. Marshall, S. P. Sisinthy, J. Panneerselvam, N. Molugulu, P. Kesharwani and H. Choudhury, *Int. J. Pharm.*, 2022, **617**, 121617, DOI: **10.1016/j.ijpharm.2022.121617**.
55 S. Zhao, Z. Chen, J. Zheng, J. Dai, W. Ou, W. Xu, Q. Ai, W. Zhang, J. Niu, K. Mai and Y. Zhang, *Fish Shellfish Immunol.*, 2019, **92**, 181–187, DOI: **10.1016/j.fsi.2019.06.004**.
56 O. M. E. Abdel-Salam, E. R. Youness, N. A. Mohammed, S. M. Y. Morsy, E. A. Omara and A. A. Sleem, *J. Med. Food*, 2014, **17**, 588–598, DOI: **10.1089/jmf.2013.0065**.
57 J. Berlanga-Acosta, J. Fernandez-Montequin, C. Valdes-Perez, W. Savigne-Gutierrez, Y. Mendoza-Mari, A. Garcia-Ojalvo,

V. Falcon-Cama, D. Garcia Del Barco-Herrera, M. Fernandez-Mayola, H. Perez-Saad, E. Pimentel-Vazquez, A. Urquiza-Rodriguez, M. Kulikovsky and G. Guillen-Nieto, *BioMed Res. Int.*, 2017, **2017**, 2923759, DOI: **10.1155/2017/2923759**.

58 S. Ogino, N. Morimoto, M. Sakamoto, C. Jinno, T. Taira and S. Suzuki, *J. Surg. Res.*, 2016, **201**, 446–454, DOI: **10.1016/j.jss.2015.11.027**.

59 S. Shafaie, S. Andalib, H. Shafaei, A. Montaseri and M. Tavakolizadeh, *Int. J. Mol. Cell Med.*, 2020, **9**, 234–246, DOI: **10.22088/IJMCM.BUMS.9.3.234**.

60 J. Hardwicke, R. Moseley, P. Stephens, K. Harding, R. Duncan and D. W. Thomas, *Mol. Pharmaceutics*, 2010, **7**, 699–707, DOI: **10.1021/mp9002656**.

61 S. Jeong, B. Kim, H. Lau and A. Kim, *Pharmaceutics*, 2019, **11**(10), 530, DOI: **10.3390/pharmaceutics11100530**.

62 L. Mehra, S. Mehra, N. Tiwari, T. Singh, H. Rawat, S. Belagavi, A. Jaimini and G. Mittal, *J. Biomater. Appl.*, 2022, **36**, 1346–1358, DOI: **10.1177/08853282211061821**.

63 P. Boukamp, R. T. Petrussevska, D. Breitkreutz, J. Hornung, A. Markham and N. E. Fusenig, *J. Cell biol.*, 1988, **106**, 761–771, DOI: **10.1083/jcb.106.3.761**.

64 D. Zhao, Y. Jiang, J. Sun, H. Li, X. Luo and M. Zhao, *J. Agric. Food Chem.*, 2019, **67**, 1230–1243, DOI: **10.1021/acs.jafc.8b06263**.

65 W. Chiu, T. V. Tran, S. Pan, H. Huang, Y. Chen and T. Wong, *Adv. Wound. Care.*, 2019, **8**, 476–486, DOI: **10.1089/wound.2018.0927**.

